



Tyrosyl radical in haemoglobin and haptoglobin-haemoglobin complex: how does haptoglobin make haemoglobin less toxic?

Dimitri A. Svistunenko^{1,✉}, Andreea Manole²

¹Biomedical EPR Facility, School of Life Sciences, University of Essex, Colchester, Essex CO4 3SQ, UK;

²Laboratory of Genetics, The Salk Institute for Biological Studies, La Jolla, CA 92037, USA.

Abstract

One of the difficulties in creating a blood substitute on the basis of human haemoglobin (Hb) is the toxic nature of Hb when it is outside the safe environment of the red blood cells. The plasma protein haptoglobin (Hp) takes care of the Hb physiologically leaked into the plasma – it binds Hb and makes it much less toxic while retaining the Hb's high oxygen transporting capacity. We used Electron Paramagnetic Resonance (EPR) spectroscopy to show that the protein bound radical induced by H₂O₂ in Hb and Hp-Hb complex is formed on the same tyrosine residue(s), but, in the complex, the radical is found in a more hydrophobic environment and decays slower than in unbound Hb, thus mitigating its oxidative capacity. The data obtained in this study might set new directions in engineering blood substitutes for transfusion that would have the oxygen transporting efficiency typical of Hb, but which would be non-toxic.

Keywords: blood substitute, EPR, haemoglobin toxicity, haptoglobin, HBOC, protein-bound radical, TRSSA

Introduction

In the search for artificial blood for transfusion, one of the avenues for exploration is creation of a non-toxic haemoglobin-based oxygen carrier (HBOC)^[1]. The oxygen transporting protein haemoglobin (Hb) must be in the ferrous haem (Fe²⁺) oxidation state to be able to transport O₂. Hb, however, is prone to spontaneous oxidation to the ferric (Fe³⁺) state by the very oxygen which is meant to transport^[2]. The ferric state of Hb, apart from being deprived of the protein's main function of binding oxygen, is a powerful pro-

oxidant that readily reacts with hydrogen peroxide H₂O₂, continuously formed in living systems. This reaction can initiate damage, *via* a free radical mechanism, to other biological molecules, particularly *via* triggering chain reactions in lipid oxidation^[3–4]. This intrinsic Hb's toxicity is controlled in the red blood cells (RBC), the protein's natural location, by the enzyme systems aimed at keeping Hb reduced and H₂O₂ continuously removed^[5–6]. However, if Hb is used as an oxygen carrier outside the protective environment of RBC, the toxicity of Hb becomes an important issue. The plasma protein haptoglobin (Hp)

✉ Corresponding author: Dimitri A. Svistunenko, Biomedical EPR Facility, School of Life Sciences, University of Essex, Colchester, Essex CO4 3SQ, UK. Tel/Fax: +44-1206-873149/+44-1206-872592, E-mail: svist@essex.ac.uk.

Received 08 September 2018, Revised 27 November 2018, Accepted 01 March 2019, Epub 15 May 2019

CLC number: R457.1, Document code: A

The authors reported no conflict of interests.

This is an open access article under the Creative Commons Attribution (CC BY 4.0) license, which permits others to distribute, remix, adapt and build upon this work, for commercial use, provided the original work is properly cited.

irreversibly binds Hb that leaks from damaged RBC^[7], to facilitate its removal by the macrophages. The interaction of the cysteine-rich CD163 receptor, located in the macrophages membrane^[8], with the Hp-Hb complex (or with unbound Hb when Hp in plasma is exhausted^[9]) activates the protein's internalisation and catabolism by the phagocyte. While such facilitation of removal of free Hb from the blood flow is recognized as the primary function of Hp^[10], it has also been reported that Hb binding to Hp results in a hindered Hb reactivity in the blood thus reducing significantly the overall oxidative damage to tissues and organs^[11-12]. Interestingly, this does not affect the ferrous Hb's ability of binding O₂^[13]. The most likely explanation of such a protective effect must be in the Hp's ability to change kinetics of free radical formation in Hb and free radical character transfer through the Hb molecule and onto other molecules. Mechanistic details of such effects are not clear.

It has been shown by a combination of spin trapping and mass-spectrometry methods that Hp binding shifts the Hb inflicted oxidative damage from other molecules to the Hb molecule itself, mostly affecting the β -subunit of Hb^[14].

Low temperature Electron Paramagnetic Resonance (EPR) spectroscopy has been used before to detect directly and analyze the free radicals in Hb and Hp-Hb complex^[15-16], and it was suggested that Hp, when bound to Hb, makes the peroxide-induced radical on Hb less reactive^[15]. However, no mechanism was proposed for such diminished reactivity. Significantly more information about Hb-bound radicals can be obtained from their room temperature EPR spectra, known to exhibit a better resolution between spectral components^[17]. Therefore, our aim was to detect and compare the EPR spectra of the H₂O₂-induced free radicals in free Hb and in the Hp-Hb complex at room temperature. If the line shapes of such spectra are different, the differences will be described quantitatively by different spectra simulation parameters. The latter will be translated into structural differences.

We used three new methodological approaches, line shape correction for rapidly accumulated EPR spectra, updated Tyrosyl Radical Spectra Simulation Algorithm (TRSSA^[18]) and radical site assignment on the basis of multiple structure files analysis, (see Materials and methods), to demonstrate that the radicals in the two systems are likely to be formed on the same amino acid residues of Hb, Tyr42 of α -subunit and Tyr130 of β -subunits, but since the radical EPR spectrum in the Hp-Hb complex is consistent with a significantly higher hydrophobicity of the

radical's microenvironment than in free Hb, we put forward a hypothesis that Hp binding to Hb affects the balance between primary radical species on Hb, shifting it in favor of the more hydrophobic, β Tyr130 radical. The free radical in the complex, weaker engaged in H-bonding to other residues or water molecules, will have diminished reactivity and that might play the causative role in lower oxidative capacity of Hb when it is bound to Hp. Understanding the mechanism of this effect is important for development of a non-toxic HBOC.

Materials and methods

Solutions

Human Hb was purified from blood donated by a volunteer as described in^[19] followed by a catalase contamination removal procedure^[20]. Human Hp (phenotype 1-1), H₂O₂ and all buffer components were purchased from Sigma-Aldrich (USA). Hb concentration in the stock was determined from optical absorbance at 435 nm in a Hb sample reduced by an excess of sodium dithionite by using molar extinction coefficient $\epsilon_{435}=121\ 000\ (\text{mol/L}\cdot\text{cm})^{-1}$ ^[21]. H₂O₂ concentration was determined by using $\epsilon_{240}=43.6\ (\text{mol/L}\cdot\text{cm})^{-1}$ ^[22]. In a typical mixing experiment, 1 mg lyophilized Hp (as supplied by Sigma) was dissolved in 150 μL of 50 mmol/L KPi buffer. To this solution, or a 150 μL volume of pure buffer in an unbound Hb experiment, a volume of 35 μL of the stock metHb (ferric Fe³⁺ Hb) solution in 10 mmol/L KPi buffer (pH 7.4) was added, and the total volume of 185 μL was taken by one of the syringes of the mixing device (*vide infra*). The other syringe was filled with 185 μL of a H₂O₂ solution in the buffer (50 mmol/L) used to dissolve Hp. The buffers were bubbled with nitrogen gas for 15 minutes before use in making the protein and peroxide solutions.

The comparison of the free radicals in Hb and Hp-Hb complex was performed for the Hb or Hp-Hb concentration of 260 $\mu\text{mol/L}$ by haem, before 1:1 by volume mixing with peroxide. This concentration corresponds, for approximate haemoglobins molecular weight of 64 000 to 4.15 mg/mL. With the final concentration of Hp in the same solution of 5.41 mg/mL, the ratio equals to 0.77 mg Hb/mg Hp which is above the binding capacity value of 0.5 as given by Sigma-Aldrich indicating that all Hp in the solution should be bound to Hb.

EPR measurements, the use of the Teslameter

All EPR spectra were measured on a Bruker EMX

EPR spectrometer (X-band) equipped with a spherical high quality resonator ER 4122 and a Bruker AquaX system for liquid sample measurements. A home-made mixing device (150 μ L minimal intake to each of two 1 mL syringes; dead volume 80 μ L) was attached to the AquaX line. To minimize the dead volume of AquaX, the inlet tubing was shortened to 1 cm. The total dead volume of the mixing device, plus AquaX was about 100 μ L. After each mixing experiment, the AquaX line was washed with 10 mL of water, 5 mL of ethanol and dried using compressed air cleaned on a cotton filter. The mixing device was washed and dried separately.

When performing a mixing experiment, the 2D spectra accumulation regime (*Acquisition* application of WinEPR for Windows 7, Bruker Analytik GmbH) was employed, when a pre-set number of spectra were measured consecutively. An example of several "slices" of a 2D spectrum set is given in **Fig. 1**. A 2D scan was started first, then the two plungers of the mixing device were pushed up to fill the AquaX cell with a reaction mixture – this moment is clearly seen in the first spectrum as an abrupt shift in the baseline. The instrumental settings used to record a 2D spectrum set were: microwave frequency $\nu_{MW}=9.862$

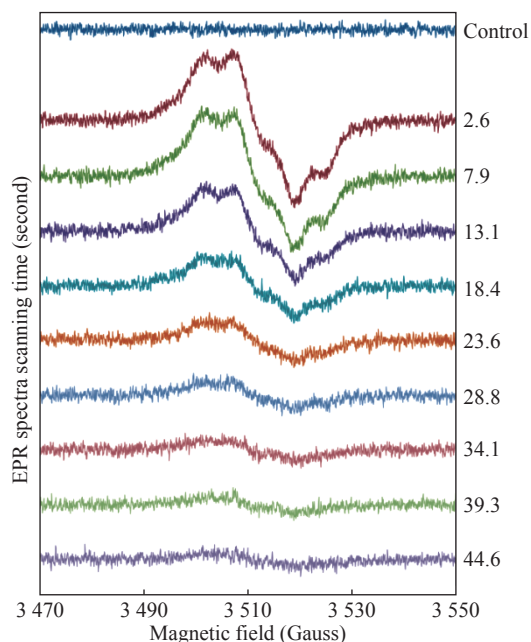


Fig. 1 Consecutively measured spectra of 340 μ mol/L methHb (by haem) reacting with 1360 mmol/L H_2O_2 (a 4-fold excess of peroxide over haem). Both of these concentrations are final (in the mixture). The EPR measurements were performed at room temperature, pH 7.5 (75 mmol/L NaPi). Each scan lasted for 5.243 seconds, the time assigned to each spectrum (rounded down and indicated) corresponds to the middle point of each scan. The solutions were mixed and pushed up into the AquaX cell in the resonator at the end of the first, control scan.

GHz; microwave power $P_{MW}=2.012$ mW; modulation amplitude $A_M=3$ G; modulation frequency $\nu_M=100$ kHz; field width (as set, *vide infra*) $\Delta H=100$ G; scan time $ST=5.243$ seconds; time constant $\tau=2.56$ milliseconds. At a spectrum field width ΔH set to 100 G, expected time of passing a distance of 1 G (a width of a typical spectral feature to be resolved) was thus 1 G / (100 G / 5.243 seconds)=52.4 milliseconds which was about 20 times greater than $\tau=2.56$ milliseconds.

The EPR spectra scanning time as short as 5.243 seconds resulted in the spectra line shape distortion *via* the self-inductance effect, when the actual magnetic field is delayed with respect to a steadily increasing voltage applied to the magnet's coils causing the actual field width to be smaller than the width set on the instrument. Thus, the field values cannot be automatically translated from the voltage, and a direct and independent field measurement is required. This was achieved by using a Teslameter (Bruker Ltd) that was monitoring the magnetic field during spectra measurements. **Fig. 2** shows that while the field width is set to 100 G, the final point in the spectrum corresponds to a smaller field increment if the spectrum is acquired rapidly. The measurements enabled by the Teslameter show that the faster the scan - the greater the difference.

Although the Teslameter measures the field at the final point of a spectrum with an impaired accuracy (the faster the scan the lower the accuracy, see **Fig. 2**) the final field itself is persistently the same and does not fluctuate with the Teslameter measurements. This has been established from a perfect correspondence of actual spectra measured many times at the same scan

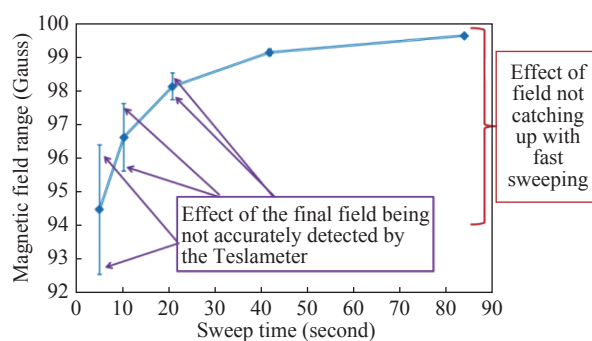


Fig. 2 Magnetic field range of a spectrum as reported by the Teslameter at different spectra scan rates. As the sweep time becomes notably shorter than 90 seconds, the field range, although always set to 100 Gauss on the spectrometer, becomes smaller. The accuracy, with which the Teslameter measures the field at the final point of the field sweep, is affected by the sweep rate – the faster the sweep, the greater the error: the error bars represent the standard deviations determined on the basis of ten runs. The field of the starting point of the spectra obtained at different scan rates was persistently the same.

rate: the spectra are superimposable to the degree of a single data point (for 2048 points per spectrum). This correspondence will collapse as soon as a different scan rate is used: the spectra measured at two different scan rates are not perfectly superimposable.

Accurate recording by the Teslameter of the magnetic field during EPR measurements is critical for accurate determination of the radicals parameters through spectral simulation, which in turn is the key for the radical site identification and for concluding the change of its environment on Hp binding.

Simulation of Tyr radical EPR spectra, TRSSA

The tyrosyl (Tyr) radical EPR spectra were simulated by SimPow6^[23] while the simulation parameters were chosen by using an updated version of TRSSA^[18] which defines all Hamiltonian parameters necessary for simulation of a Tyr radical EPR spectrum: some parameters are set invariant for all Tyr radicals, the others are defined as explicit functions of only two variables, the phenoxyl ring rotation angle θ and the electron spin density ρ_{C1} on atom C1 of the radical (**Supplementary Fig. 1**, available online). In the updated TRSSA available in the *Supplementary TRSSA2.xlsx* (all the supplementary files are available on <https://1drv.ms/u/s!ArZmAEA-E2XThrNQz79qUXuUqIrL-A?e=4fNPKw>), six previously invariant parameters are made dependable on θ . These parameters are the Euler angles for the hyperfine interaction tensors of the two β -methylene protons in a Tyr radical. (Please see details in the *Supplementary Supporting_text_figures_tables.pdf*, available online).

Radical site assignment

The analysis of the rotational conformation of tyrosines in human Hb was performed by using the on-line database^[24]. The nine Protein Data Bank (PDB) files analyzed are 2HCO^[25] (two subunits only), 1HHO^[26] (two subunits only), 2HHB^[27], 1HGA 1HGB, 1HGC^[28], 1IRD (Park & Tame, 2001; carbonmonoxy-haemoglobin at 1.25 Å resolution; no paper has been published; two subunits only), 2W6V^[29], and 3P5Q^[30] (two subunits only; α -subunit is reported up to residue 139). Overall, the five tetramers and four dimers make $5 \times 2 + 4 \times 1 = 14$ entries available for statistical analysis of a single Tyr residue in either α or β chain. The ring rotation angles φ (**Supplementary Fig. 1**, available online) in all tyrosines in the nine human Hb structure files have been determined from the atom coordinates. The φ -values have been uploaded to the database^[24]; the

server used the values to calculate the θ angles. The database further allowed ranking the tyrosines, within each structure, by proximity of the ring rotation angle θ to the values found from the EPR spectra simulations (*Supplementary PDB_files_analysis.xlsx*, available online).

Results

Optimising reaction conditions and EPR instrumental parameters

Real time detection of rapidly changing concentrations of free radicals requires optimization of the protein and peroxide concentrations, reaction's pH and temperature, as well as the EPR instrumental parameters. The comparison of the free radical formed in Hb and Hp-Hb under peroxide treatment had to be performed for the same reaction conditions. Having in mind that the low temperature EPR spectroscopy previously reported a free radical yield in the complex higher than in free Hb^[15], these conditions were chosen by screening a range of protein and H₂O₂ concentrations for unbound Hb, which is a much cheaper option to experiment on as compared to the Hp-Hb complex.

We started with 700 $\mu\text{mol/L}$ metHb, the concentration for which a liquid phase spectrum of the Tyr radical in Hb has been previously reported^[17], and worked down towards lower concentrations which would be closer to the physiological conditions of Hp interacting with Hb. Also, the radical decay is slower at lower Hb concentrations^[31], thus allowing for a longer EPR signal observation. However, as protein concentration is decreased, the EPR signal becomes smaller. This could be compensated by setting the EPR spectrometer to a higher sensitivity, for example, to a higher microwave power, higher modulation amplitude or a longer spectrum acquisition time. However, excessive modulation amplitude would affect the EPR spectrum line shape which would be unacceptable if the spectrum is meant to be simulated. A high microwave power can also affect the line shape *via* the microwave power saturation effects, as well as it can increase the temperature of the water-base samples (at the power values of greater than 5 mW). There is also a limitation to how long a spectrum acquisition can take: it should not be longer than the time of a noticeable change in the free radical concentration. The latter is a direct function of the reaction components concentrations and the pH value at which the reaction is run.

The choice of microwave power P_{MW} was made to

be 2.012 mW; the modulation amplitude A_M was chosen to be 3 G, and the individual spectrum scan rate was chosen to be 5.243 seconds.

The starting hydrogen peroxide concentration in the reaction mixture was screened within the range of 3–20 molar excess over haem, for each of the Hb concentrations tested. The choice of a 12-fold molar excess of peroxide over haem has been finally made for the experiment in which free radical will be compared in the two systems.

The pH dependence of free radical formation in metHb under H_2O_2 treatment was studied in the pH range between 5 and 8 (**Fig. 3**). The data presented in the figure were obtained by averaging 2–3 individual mixing experiments. The errors of the averages are not shown. Instead, the individual kinetics for all mixing experiments are given in **Supplementary Fig. 3** (available online). We have chosen to compare the reactions of Hb and Hp-Hb complex with H_2O_2 in a KPi buffer at pH 7.4.

All spectra were recorded at ambient temperature. At an early stage of experiments, the EPR measurements were taken after reaction components were pre-incubated at 37 °C for 5 minutes. This produced a significant random error in radical yield and kinetics, possibly due to uncontrolled cooling of the reaction components (in separate syringes) and the reaction mixture (in the mixing device and the AquaX capillaries) once the solutions were out of the thermostat. Therefore, it has been decided to run all experiments at room temperature (22 °C).

Two systems measured at identical conditions: average spectra

Fig. 4 shows room temperature EPR spectra of the

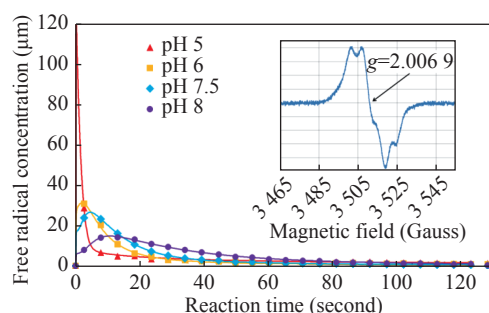


Fig. 3 Kinetic dependences of the tyrosyl free radical in the mixtures of 340 $\mu\text{mol/L}$ human metHb and 1.36 mmol/L H_2O_2 (both concentrations are final), at different pH values. The symbols in each dependence represent average values of two or three similar experiments shown individually in **Supplementary Fig. 3**, available online. The lines represent a solution obtained by the kinetic model developed for a different haemoglobin system^[37] and are therefore for illustrative purpose only. *Inset* shows an EPR spectrum of the tyrosyl radicals obtained by averaging 13 individual spectra specified in **Supplementary Fig. 3**, available online.

free radical formed in Hb and the Hp-Hb complex on H_2O_2 addition, under similar reaction and instrumental conditions. Initial spectra of different mixing experiments (2 to 4 first spectra of different 2D spectral sets) and their averaged spectra are shown for the two systems. Both averaged spectra represent typical^[18] Tyr radical EPR line shapes, and the Hb radical has indeed been assigned to a tyrosine before^[17,32].

The kinetics of the Tyr radical concentration in Hb

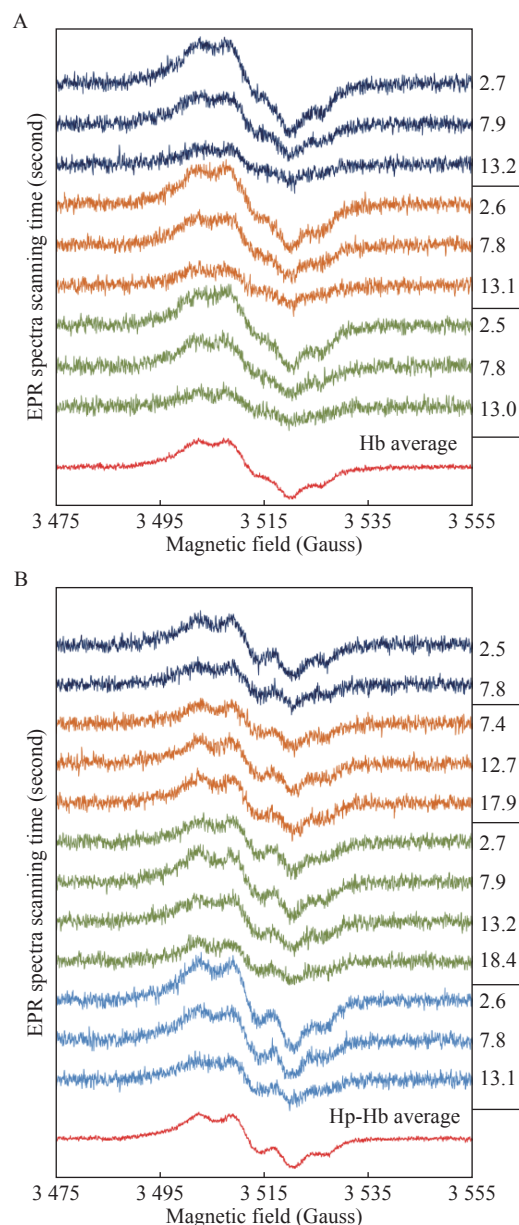


Fig. 4 Liquid phase EPR spectra of Tyr radical in Hb and Hp-Hb. A: The first EPR scans of three independent experiments of mixing 130 $\mu\text{mol/L}$ Hb (by haem) with a 12-fold excess H_2O_2 (1 558 $\mu\text{mol/L}$) at pH 7.4 (KPi), the time elapsed after mixing is indicated. The spectrum at the bottom is an average of the spectra above. B: Similar to a), but for four independent series of 130 $\mu\text{mol/L}$ Hp-Hb (by Hb haem) mixed with a 12-fold excess H_2O_2 .

and in the complex are different (**Fig. 5**): the free radical disappearance is clearly slower in the complex than in the unbound Hb.

Simulation of the two spectra: similar angles, different spin densities on C1

The average EPR spectra of the free radical in the Hb and Hp-Hb systems (**Fig. 4**), although exhibiting significant differences in the line shape, are both typical of Tyr radicals. To simulate these spectra, an updated version of previously published^[18] TRSSA (see part 2.3 in Materials and methods), has been used. **Fig. 6** shows that both line shapes are simulated for practically the same angle θ ($\theta=53.0^\circ$ in Hb and $\theta=54.3^\circ$ in Hp-Hb). However, the other TRSSA input parameter, ρ_{C1} , is significantly lower in the Hp-Hb Tyr radical, 0.360, as compared to the value of 0.405 in the unbound Hb radical. When the two ρ_{C1} values are placed on a ρ - g chart (**Fig. 7**), which is a useful way of showing the relationship between ρ_{C1} and three principal g -values of a Tyr radical^[33], it becomes clear that the spread of the three g -values of the Tyr radical in Hb increases significantly on Hp binding indicating that the radical's microenvironment changes towards more hydrophobic. We note that the microenvironment of the Tyr radical in the Hp-Hb complex is only marginally different from the most hydrophobic environment known for Tyr radicals (the ρ_{C1} value is at the bottom of the shaded area, **Fig. 7**)^[18, 34].

Assignment of the radicals to specific sites: α Tyr42 and β Tyr130 are the most probable locations

The EPR spectra of the Tyr radical in both unbound Hb and Hp-Hb complex were simulated for very close values of the tyrosine ring rotation angle θ , 53.0° , and 54.3° , respectively. This is a strong indication that the radicals are formed on the same residues in the two

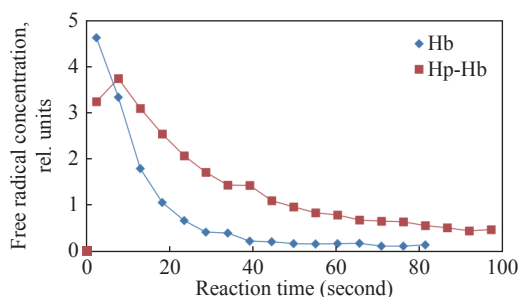


Fig. 5 Kinetic dependences of the tyrosyl radical in the Hb+H₂O₂ and Hp-Hb+H₂O₂ systems. The concentrations of Hb or Hp-Hb complex in the mixtures were 130 μ mol/L, the peroxide concentration was 1.56 mmol/L, pH 7.4 (the same experiments as in **Fig. 4**). Each data point is an average of three independent mixing experiments detailed in **Supplementary Fig. 4**, available online.

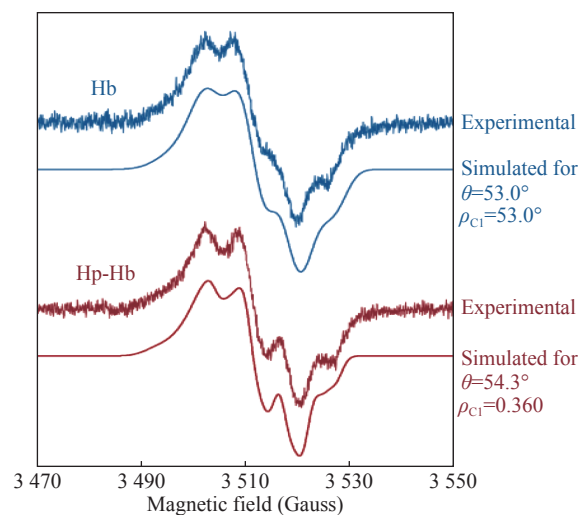


Fig. 6 The averaged EPR spectra of the free radicals formed under H₂O₂ addition to Hb and to the Hp-Hb complex (the same as shown in **Fig. 4**) and their simulations as tyrosyl radical EPR signals. The simulation parameters, reported in **Supplementary Table 1** and **Supplementary Table 2** (available online), were found by TRSSA for the inputs indicated.

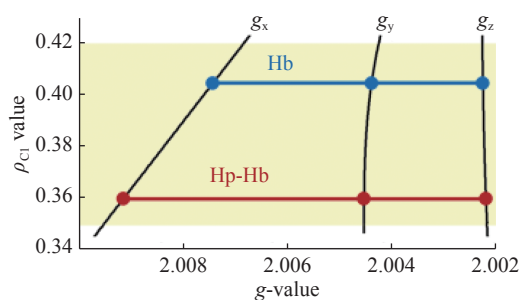


Fig. 7 A ρ - g chart^[18,33] showing the principal g -factor sets for the tyrosyl radicals in Hb and Hp-Hb. The three dependences labelled g_x , g_y and g_z are the functions adopted in TRSSA^[18]. The three g -values on these dependences correspond to the ρ_{C1} values found from the simulations, 0.405 and 0.360. The shaded area corresponds to the range of spin density on C1 in all known tyrosyl radicals^[18].

systems. We then employed the database of rotational orientation θ of the ring in tyrosines^[24] and analyzed all tyrosines in nine human haemoglobin crystal structures (details of the structure files are given in part 2.4 in Materials and methods). Thus, while previous site assignments of radicals in different proteins based on this method^[15,17,18,35–37] relied on analyses of a single PDB file, here we present the result of analysis of several related structures which gives an answer with a statistical confidence. We ranked all of the tyrosines by the proximity of their average (over nine structures) angle θ to the values of either 53.65° or 66.35° (see the *Human structures spreadsheet* in *Supplementary PDB_files_analysis.xlsx*, available online). The first value of 53.65° is an

average of the two θ angles, 53.0° and 54.3° , obtained from the simulations of the EPR spectra of the radical in Hb and Hp-Hb (**Fig. 6**). The other angle, 66.35° , is its complementary value—the sum of the two is $66.35^\circ + 53.65^\circ = 120^\circ$. The two complementary angles yield identical EPR spectra simulation parameters^[38], and therefore all tyrosines should be analyzed for proximity to either of the two possible angles. The data reported in the *Human structures* spreadsheet have been re-grouped to form blocks of data for individual Tyr residues across different structures and sorted by the proximity of angle θ to the two different target values, to $\theta = 53.65^\circ$ (spreadsheet *53.65_sorted*) and to $\theta = 66.35^\circ$ (spreadsheet *66.35_sorted* in *PDB_files_analysis.xlsx*). The average values and standard deviations were determined for specific residues (on the array of several structures) and compared to the two 'target values' (**Fig. 8**). The figure shows that the residue Tyr42 on the α -chain has the ring rotation angle most close to one of the two complimentary values of θ_{target} obtained from the simulation (the difference $|\theta - \theta_{\text{target}}|$ is the lowest for α Tyr42 and $\theta_{\text{target}} = 53.65^\circ$).

Discussion

Updated TRSSA provides more accurate spectra simulation parameters

The simulation of Tyr free radical EPR spectra in Hb and Hp-Hb complex was performed with the use of an updated TRSSA, which now allows calculation of the Euler angles for the hyperfine interactions tensors A of the two methylene protons as functions of the ring rotation angle θ , albeit for a limited θ interval of $30^\circ \leq \theta \leq 60^\circ$ (*Supplementary Supporting_*

text_figures_tables.pdf, available online).

In an EPR spectrum simulation, the anisotropic g -tensor must be sterically related to the anisotropy of the hyperfine interaction of the unpaired electron spin with paramagnetic nuclei (the protons in the Tyr radical case). This is usually achieved in the simulation procedure by specifying three Euler angles Φ_1, Φ_2, Φ_3 for each proton that define a three-step rotation of the hyperfine interaction tensor (A -tensor) to align its principal axes with the principal axes of the g -tensor. For the four ring protons, H_{C2}, H_{C3}, H_{C5} and H_{C6} , the Euler angles have been suggested from the symmetry considerations^[39], further corrected^[40] and later confirmed by the density function theory calculations^[33]: just one rotation, within the plane of the ring, is sufficient to align the two sets of principal axes. Symmetrical ring protons (H_{C2} and H_{C6} ; H_{C3} and H_{C5}) will have the same values of the Euler angle but with opposite signs. Obviously, rotational conformation of the ring does not affect the Euler angles for A - and g -tensors for the ring protons (Φ_1, Φ_2, Φ_3 do not depend on θ for the protons on C2, C3, C5, and C6).

The situation is more complex for the β -methylene protons which are off the ring's plane and do not rotate with the ring. While it is clear that the Euler angles should be changing with the ring rotation angle in a harmonic fashion, there are no intuitive indications of how the A -tensors are arranged with respect to the ring (which is linked to the g -tensor) and no experimental approach exists to find this out. Possibly because of this, it is quite often that the Euler angles for the methylene protons are not indicated in the literature, thus incorrectly assuming that the principal A -values (measured experimentally and shown to form almost

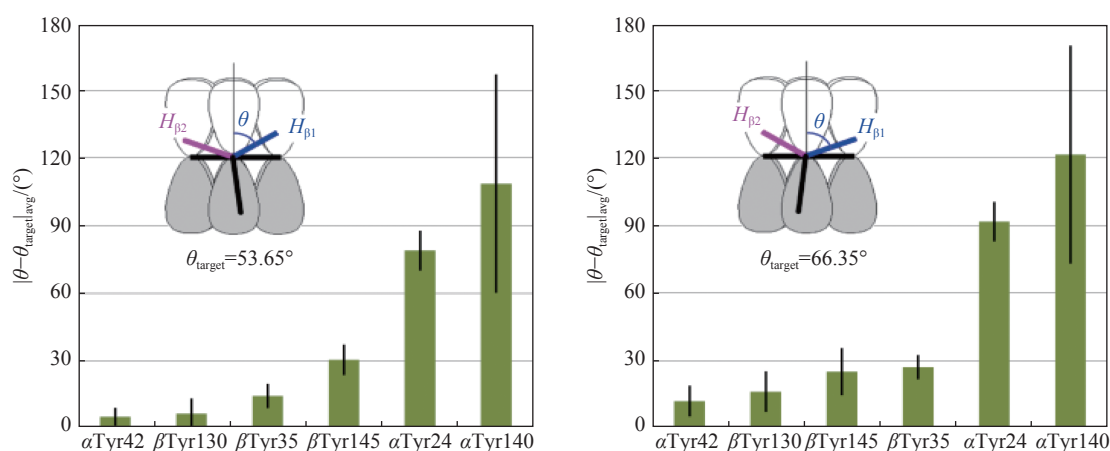


Fig. 8 The closeness of the phenol ring rotation angle θ in the six tyrosines in Hb to the target value of either 53.65° (average of the 53° and 54.3° angles reported in **Fig. 6**) or its complementary angle of 66.35° (see **Materials and methods**). The average $|\theta - \theta_{\text{target}}|$ differences and their standard deviations are found on the basis of 9 structure files as specified in **Materials and methods**.

axial tensors)^[41] are collinear with the principal values of the g -tensor. This cannot be right, and the approximation "worked" for several previous simulations at the expense of errors introduced in other EPR spectra simulation parameters. The original version of TRSSA, based on previous work performed in the field, also assumed the three Euler angles for each of the two methylene protons to be zeros.

Modified TRSSA presented here makes a first step in defining the Euler angles for the methylene protons' A -tensors. Therefore, it provides more accurate simulations thus yielding more accurate values of θ and ρ_{C1} for the radicals in the Hb and Hp-Hb systems, for both of which the θ is expected within the interval of $30^\circ \leq \theta \leq 60^\circ$. As the next step, a version of TRSSA that would have Euler angles defined on the full range of possible values $0^\circ \leq \theta \leq 360^\circ$ is being developed now and will be reported elsewhere.

Radical locations are likely to be the same in Hb and in the complex

If the two free radical EPR spectra reported here, in unbound Hb and Hp-Hb complex, are caused by a single Tyr radical species, the radical site is likely to be the same in the two systems. This follows from the closeness of the values of θ for the two simulated EPR spectra (**Fig. 6**). It is more probable that practically the same angle in the two systems is not a coincidence but a manifestation of the fact that Hp-bound Hb reacts with H_2O_2 *via* the same mechanism as unbound Hb does. Such a conjecture is supported by the ability of the Hp-Hb complex to bind NO and O_2 ^[13,42] which means that the oxygen binding site, the 6-th haem coordination position, is unaffected by Hp binding. On the other hand, an alternative possibility, that the experimental spectra in **Fig. 6** are caused by more than one Tyr radical, with the simplest scenario - by radicals at two different Tyr sites, should be also considered (*vide infra*).

Location of the radical(s)

The analysis of rotational orientations of tyrosine rings in nine human Hb structures has shown that Tyr42 is the most probable residue to host the radical. Interestingly, α Tyr42 is located close to the haem edge, and the formation of free radicals on structurally homologous tyrosines has been demonstrated for several globins treated with H_2O_2 : in horse, sperm whale and human myoglobins (Tyr103)^[36], in leghaemoglobin (Tyr133)^[43] and in dehaloperoxidase haemoglobin (Tyr34)^[37] as well as in the Ser160Tyr variant of the haem enzyme ascorbate peroxidase (Tyr160)^[44]. It is possible that a Tyr in this position in

globins is a valuable evolutionary development destined to stabilize a radical on the protein and thus to minimize the damage the free radical might impose on other molecules.

Is it feasible that the primary free radical we see in Hb is located only on the α -chains and not being formed (or not being stable enough for us to detect it) on the β -chain? We feel it would be strange if this were the case since all globins readily react with H_2O_2 , and a free radical should be formed early on the β -chains, pretty much as early as on α -chains, and later might be transferred between the chains as well^[14]. If so, it appears that β Tyr130 is the most likely candidate to host the primary radical on the β -chains as it has the second most close angle θ to the value determined from the simulation (**Fig. 8**).

Thus, while the most probable residue to host experimentally observed free radical in Hb is α Tyr42, it is also possible that the experimental EPR spectrum is caused by a superposition of EPR signals from more than a single free radical species, and if so, the tyrosines α Tyr 42 and β Tyr130 are the most probable residues to form a combination of more than one free radical species.

A lower value of ρ_{C1} in the complex

The key finding of this work is that Hp binding results in a significant decrease of the spin density on atom C1 of the tyrosyl radical formed under peroxide treatment (**Fig 7**). The ρ_{C1} value in tyrosyl radicals is in inverse correlation with the g_x value, and both have been linked to the electronegativity/hydrophobicity of the radical's microenvironment^[34,45]: the low values of ρ_{C1} correspond to a hydrophobic environment^[46], while the high ρ_{C1} are associated with electronegative environment and a possibility of a strong hydrogen bond formation^[34]. Therefore, **Fig. 7** demonstrates that when Hb is bound to Hp, the radical's microenvironment turns significantly hydrophobic as compared to the hydrophilic environment of the radical in unbound Hb. This makes sense if one of the effects of Hp binding is a decreased oxidative capacity of Hb: any protein bound radical would become less reactive if its microenvironment changes to more hydrophobic. This would not make it easier for the radical to access the hydrophobic tails of lipids inside bilayer membranes since the hydrophobic microenvironment of the radical is a relatively small region inside a much larger protein complex. But this would certainly make the lifetime of the protein radical longer, thus delaying any possible free radical character transfer through the protein complex onto cell components, particularly to membrane lipids

causing chain reaction of lipid peroxidation *via* a free radical mechanism.

It is tempting to suggest that Hp, when binding to Hb, physically insulates the radical site on Hb from the bulk solution. This, however, does not seem to be the case as can be judged from two available crystal structures of Hp-Hb complex - for the porcine proteins^[47] and the human proteins^[48–49]. In both cases, Hp binds an Hb $\alpha\beta$ -dimer over the same extensive region that is involved in forming a tetramer of two $\alpha\beta$ -dimers, showing α Tyr42 pretty much solvent exposed. In contrast, β Tyr130 (or β Phe130 in porcine Hb) is buried inside β subunit.

This arrangement of these two key residues involved in the analysis allows the following hypothesis to be put forward. In both unbound Hb and Hp-Hb complex, experimentally detected free radical EPR spectra, with a half-life of about 15 s (Hb) and 30 s (Hp-Hb) (**Fig. 5**) are both caused by a superposition of EPR signals from two Tyr radicals, on α Tyr42 and β Tyr130. Both these tyrosines have close rotational conformations of the ring but their microenvironments are significantly different, hydrophilic for α Tyr42 and hydrophobic for β Tyr130. Hp binding to an $\alpha\beta$ -dimer effects in a diminished yield of the α Tyr42 radical but an increased yield of the β Tyr130 radical. Such a shift of the free radical balance would explain a greater apparent hydrophobicity of the radical environment detected in the Hp-Hb complex, as well as its greater stability (**Fig. 5**) which could be one of the reasons for the complex's lower oxidative toxicity compared to unbound Hb.

In conclusion, thoroughly analyzed room temperature EPR spectra of the Tyr radicals formed in Hb and Hp-Hb complex, under peroxide treatment, revealed that the radical (or the radicals) exhibit the same, in the two systems, rotational conformation of the tyrosine ring, which makes it highly probable that Hp binding does not affect the location of the radical(s) formed in Hb on reaction with H₂O₂. However, the Hp binding strongly affects the microenvironment of the radical(s) - it changes from rather hydrophilic to strongly hydrophobic. Such conformational change induced by Hp would make the radical less reactive, which is confirmed by slower kinetics of radical disappearance in the complex.

If the experimental EPR spectrum is caused by a single free radical site, the most likely location of the radical is α Tyr42 and the effect of Hp binding is in changing the hydrogen bond network around the radical site, making the H-bonds weaker. If, however, the observed spectrum is a superposition of more than one type Tyr radical EPR signals, then the two most

likely sites are α Tyr42 and β Tyr130, and the Hp binding to Hb shifts the balance between the two radicals towards an increase of the contribution of the β Tyr130 radical.

The findings reported here might be useful in engineering new human Hb variants or protein-protein complexes that would have effective oxygen transporting efficiency, necessary for the development of new HBOCs, but which would have their intrinsic oxidative capacity hindered.

Acknowledgments

This work was supported by the Biomedical EPR Facility of the University of Essex. We appreciate computational time granted by the EPSRC funded UK National Service for Computational Chemistry Software (NSCCS, 1996-2017), Imperial College London.

References

- [1] Natanson C, Kern SJ, Lurie P, et al. Cell-free hemoglobin-based blood substitutes and risk of myocardial infarction and death: a meta-analysis[J]. *JAMA*, 2008, 299: 2304–2312.
- [2] Weiss JJ. Nature of the Iron-Oxygen Bond in Oxyhaemoglobin[J]. *Nature*, 1964, 202: 83–84.
- [3] Gutteridge JM. The antioxidant activity of haptoglobin towards haemoglobin-stimulated lipid peroxidation[J]. *Biochim Biophys Acta*, 1987, 917: 219–223.
- [4] Reeder BJ, Svistunenko DA, Cooper CE, et al. The radical and redox chemistry of myoglobin and hemoglobin: from *in vitro* studies to human pathology[J]. *Antioxid Redox Sign*, 2004, 6: 954–966.
- [5] Blisard KS, Mieval JJ. Role of NADPH and the NADPH-dependent methemoglobin reductase in the hydroxylase activity of human erythrocytes[J]. *Arch Biochem Biophys*, 1981, 210: 762–769.
- [6] Deisseroth A, Dounce AL. Catalase: Physical and chemical properties, mechanism of catalysis, and physiological role[J]. *Physiol Rev*, 1970, 50: 319–375.
- [7] Hwang PK, Greer J. Interaction between hemoglobin subunits in the hemoglobin-haptoglobin complex[J]. *J Biol Chem*, 1980, 255: 3038–3041.
- [8] Kristiansen M, Graversen JH, Jacobsen C, et al. Identification of the haemoglobin scavenger receptor[J]. *Nature*, 2001, 409: 198–201.
- [9] Schaer DJ, Schaer CA, Buehler PW, et al. CD163 is the macrophage scavenger receptor for native and chemically modified hemoglobins in the absence of haptoglobin[J]. *Blood*, 2006, 107: 373–380.
- [10] Moestrup SK, Moller HJ. CD163: a regulated hemoglobin scavenger receptor with a role in the anti-inflammatory response[J]. *Ann Med*, 2004, 36: 347–354.

- [11] Lim YK, Jenner A, Ali AB, et al. Haptoglobin reduces renal oxidative DNA and tissue damage during phenylhydrazine-induced hemolysis[J]. *Kidney Int*, 2000, 58: 1033–1044.
- [12] Schaer CA, Deuel JW, Bittermann AG, et al. Mechanisms of haptoglobin protection against hemoglobin peroxidation triggered endothelial damage[J]. *Cell Death Differ*, 2013, 20: 1569–1579.
- [13] Chiancone E, Antonini E, Brunori M, et al. Kinetics of the reaction between oxygen and haemoglobin bound to haptoglobin[J]. *Biochem J*, 1973, 133: 205–207.
- [14] Vallelian F, Garcia-Rubio I, Puglia M, et al. Spin trapping combined with quantitative mass spectrometry defines free radical redistribution within the oxidized hemoglobin: haptoglobin complex[J]. *Free Radic Biol Med*, 2015, 85: 259–268.
- [15] Cooper CE, Schaer DJ, Buehler PW, et al. Haptoglobin binding stabilizes hemoglobin ferryl iron and the globin radical on tyrosine b145[J]. *Antioxid Redox Signal*, 2013, 18: 2264–2273.
- [16] Mollan TL, Jia Y, Banerjee S, et al. Redox properties of human hemoglobin in complex with fractionated dimeric and polymeric human haptoglobin[J]. *Free Radic Biol Med*, 2014, 69: 265–277.
- [17] Svistunenko DA, Dunne J, Fryer M, et al. Comparative study of tyrosine radicals in hemoglobin and myoglobins treated with hydrogen peroxide[J]. *Biophys J*, 2002, 83: 2845–2855.
- [18] Svistunenko DA, Cooper CE. A new method of identifying the site of tyrosyl radicals in proteins[J]. *Biophys J*, 2004, 87: 582–595.
- [19] Antonini E, Brunori M *Hemoglobin and myoglobin in their reactions with ligands*. North-Holland Pub. Co., Amsterdam, 1971, 436 pp.
- [20] Bonaventura J, Schroeder WA, Fang S. Human erythrocyte catalase: an improved method of isolation and a reevaluation of reported properties[J]. *Arch Biochem Biophys*, 1972, 150: 606–617.
- [21] Antonini E. Interrelationship between Structure and Function in Hemoglobin and Myoglobin[J]. *Physiol Rev*, 1965, 45: 123–170.
- [22] Hugo M, Turell L, Manta B, et al. Thiol and sulfenic acid oxidation of AhpE, the one-cysteine peroxiredoxin from *Mycobacterium tuberculosis*: kinetics, acidity constants, and conformational dynamics[J]. *Biochemistry*, 2009, 48: 9416–9426.
- [23] Nilges MJ, Matteson K, Bedford RL (2007) SIMPOW6: a software package for the simulation of ESR powder-type spectra. In: *ESR Spectroscopy in Membrane Biophysics. Biological Magnetic Resonance*. Vol. 27, 261–281 pp. Springer.
- [24] Svistunenko D (2004) *Tyrosine residues in different proteins: Phenol ring rotation angle database* (<https://svistunenko.essex.ac.uk/lev1/tyrdb/home.shtml>).
- [25] Baldwin JM. The structure of human carbonmonoxy haemoglobin at 2.7 Å resolution[J]. *J Mol Biol*, 1980, 136: 103–128.
- [26] Shaanan B. Structure of human oxyhaemoglobin at 2.1 Å resolution[J]. *J Mol Biol*, 1983, 171: 31–59.
- [27] Fermi G, Perutz MF, Shaanan B, et al. The crystal structure of human deoxyhaemoglobin at 1.74 Å resolution[J]. *J Mol Biol*, 1984, 175: 159–174.
- [28] Liddington R, Derewenda Z, Dodson E, et al. High resolution crystal structures and comparisons of T-state deoxyhaemoglobin and two liganded T-state haemoglobins: T(α-oxy)haemoglobin and T(met)haemoglobin[J]. *J Mol Biol*, 1992, 228: 551–579.
- [29] Savino C, Miele AE, Draghi F, et al. Pattern of cavities in globins: the case of human hemoglobin[J]. *Biopolymers*, 2009, 91: 1097–1107.
- [30] Yi J, Thomas LM, Richter-Addo GB. Structure of human R-state aquomethemoglobin at 2.0 Å resolution[J]. *Acta Crystallogr Sect F Struct Biol Cryst Commun*, 2011, 67: 647–651.
- [31] Svistunenko DA, Reeder BJ, Wilson MT, et al. Radical formation and migration in myoglobins[J]. *Prog React Kinet Mech*, 2003, 28: 105–118.
- [32] McArthur KM, Davies MJ. Detection and reactions of the globin radical in haemoglobin[J]. *Biochim Biophys Acta*, 1993, 1202: 173–181.
- [33] Svistunenko DA, Jones GA. Tyrosyl radicals in proteins: a comparison of empirical and density functional calculated EPR parameters[J]. *Phys Chem Chem Phys*, 2009, 11: 6600–6613.
- [34] Ivancich A, Mattioli TA, Un S. Effect of protein microenvironment on tyrosyl radicals. A high-field (285 GHz) EPR, resonance Raman, and hybrid density functional study[J]. *J Am Chem Soc*, 1999, 121: 5743–5753.
- [35] Rajagopal BS, Edzuma AN, Hough MA, et al. The hydrogen-peroxide-induced radical behaviour in human cytochrome c-phospholipid complexes: implications for the enhanced proapoptotic activity of the G41S mutant[J]. *Biochem J*, 2013, 456: 441–452.
- [36] Svistunenko DA. Reaction of haem containing proteins and enzymes with hydroperoxides: The radical view[J]. *Biochim Biophys Acta*, 2005, 1707: 127–155.
- [37] Thompson MK, Franzen S, Ghiladi RA, et al. Compound ES of dehaloperoxidase decays via two alternative pathways depending on the conformation of the distal histidine[J]. *J Am Chem Soc*, 2010, 132: 17501–17510.
- [38] Svistunenko DA, Wilson MT, Cooper CE. Tryptophan or tyrosine? On the nature of the amino acid radical formed following hydrogen peroxide treatment of cytochrome c oxidase[J]. *Biochim Biophys Acta*, 2004, 1655: 372–380.
- [39] Hoganson CW, Babcock GT. Protein-tyrosyl radical interactions in photosystem II studied by electron spin resonance and electron nuclear double resonance spectroscopy: comparison with ribonucleotide reductase and *in vitro* tyrosine[J]. *Biochemistry*, 1992, 31: 11874–11880.
- [40] Hoganson CW, Sahlin M, Sjöberg B-M, et al. Electron magnetic resonance of the tyrosyl radical in ribonucleotide reductase from *Escherichia coli*[J]. *J Am Chem Soc*, 1996, 118: 4672–4679.
- [41] Rigby SE, Nugent JH, O'Malley PJ. The dark stable tyrosine

- radical of photosystem 2 studied in three species using ENDOR and EPR spectroscopies[J]. *Biochemistry*, 1994, 33: 1734–1742.
- [42] Azarov I, He X, Jeffers A, et al. Rate of nitric oxide scavenging by hemoglobin bound to haptoglobin[J]. *Nitric Oxide*, 2008, 18: 296–302.
- [43] Davies MJ, Puppo A. Direct detection of a globin-derived radical in leghemoglobin treated with peroxides[J]. *Biochem J*, 1992, 281: 197–201.
- [44] Pipirou Z, Bottrill AR, Svistunenko DA, et al. The reactivity of heme in biological systems: autocatalytic formation of both tyrosine-heme and tryptophan-heme covalent links in a single protein architecture[J]. *Biochemistry*, 2007, 46: 13269–13278.
- [45] Un S, Gerez C, Elleingand E, et al. Sensitivity of tyrosyl radical g-values to changes in protein structure: a high-field EPR study of mutants of ribonucleotide reductase[J]. *J Am Chem Soc*, 2001, 123: 3048–3054.
- [46] Allard P, Barra AL, Andersson KK, et al. Characterization of a new tyrosyl free radical in *Salmonella typhimurium* ribonucleotide reductase with EPR at 9.45 and 245 GHz[J]. *J Am Chem Soc*, 1996, 118: 895–896.
- [47] Andersen CB, Torvund-Jensen M, Nielsen MJ, et al. Structure of the haptoglobin-haemoglobin complex[J]. *Nature*, 2012, 489: 456–459.
- [48] Stodkilde K, Torvund-Jensen M, Moestrup SK, et al. Structural basis for trypanosomal haem acquisition and susceptibility to the host innate immune system[J]. *Nat Commun*, 2014, 5: 5487.
- [49] Lane-Serff H, MacGregor P, Lowe ED, et al. Structural basis for ligand and innate immunity factor uptake by the trypanosome haptoglobin-haemoglobin receptor[J]. *Elife*, 2014, 3: e05553.

RECEIVE IMMEDIATE NOTIFICATION FOR
EARLY RELEASE ARTICLES PUBLISHED ONLINE

To be notified by e-mail when *Journal* early release articles are
published online, sign up at jbr-pub.org.cn.